What can we learn from the electromagnetic properties of hidden-charm molecular pentaquarks with single strangeness?

Fu-Lai Wang,[1,2,3,*] Hong-Yan Zhou,[1,2,†] Zhan-Wei Liu,[1,2,3,‡] and Xiang Liu[1,2,3,§]

[1]*School of Physical Science and Technology, Lanzhou University, Lanzhou 730000, China*
[2]*Research Center for Hadron and CSR Physics, Lanzhou University and Institute of Modern Physics of CAS, Lanzhou 730000, China*
[3]*Lanzhou Center for Theoretical Physics, Key Laboratory of Theoretical Physics of Gansu Province, and Frontiers Science Center for Rare Isotopes, Lanzhou University, Lanzhou 730000, China*

(Received 26 August 2022; accepted 8 September 2022; published 20 September 2022)

Inspired by the observation of the $P_{\psi s}^{\Lambda}(4459)$ and $P_{\psi s}^{\Lambda}(4338)$, we systematically investigate the magnetic moments, the transition magnetic moments, and the radiative decay behaviors of the S-wave isoscalar $\Xi_c^{(\prime)}\bar{D}^{(*)}$ molecular pentaquark states in this work. Our quantitative investigation shows that their electromagnetic properties can provide important hints to decode the inner structure of these discussed isoscalar $\Xi_c^{(\prime)}\bar{D}^{*}$ molecular pentaquarks. As a potential research issue, we suggest future experiments to focus on the electromagnetic properties of these isoscalar $\Xi_c^{(\prime)}\bar{D}^{(*)}$ molecular pentaquarks, which are a typical hidden-charm molecular pentaquark system with single strangeness.

DOI: 10.1103/PhysRevD.106.054020

I. INTRODUCTION

Since the discovery of the $X(3872)$ by the Belle Collaboration in 2003 [1], a large number of exotic hadronic states have been observed in the past two decades, which stimulated extensive discussion around them [2,2–12]. As an important part of the exotic hadron spectroscopy, the molecular state picture was extensively applied to explain them, where we have witnessed the big progress on the experimental and theoretical exploration of the hidden-charm molecular pentaquarks [2–12]. Especially, the observation of three P_{ψ}^{N} states, $P_{\psi}^{N}(4312)$, $P_{\psi}^{N}(4440)$, and $P_{\psi}^{N}(4457)$, by the LHCb Collaboration in 2019 [13], provides strong evidence to support the existence of the hidden-charm molecular pentaquarks in the hadron spectroscopy [14–20].

In 2021, LHCb reported the evidence of the $P_{\psi s}^{\Lambda}(4459)$, a candidate of the hidden-charm pentaquark with strangeness, by analyzing the $\Xi_b^- \to J/\psi\Lambda K^-$ process [21], which can be viewed as the $\Xi_c\bar{D}^{*}$ molecular pentaquark state [22–47]. As indicated by LHCb, the $P_{\psi s}^{\Lambda}(4459)$ state can be as a double-peak structure [21] similar to the case for the $P_{\psi}^{N}(4450)$ enhancement structure [48], which can be replaced by two substructures $P_{\psi}^{N}(4440)$ and $P_{\psi}^{N}(4457)$ [13]. Very recently, LHCb reported the observation of the $P_{\psi s}^{\Lambda}(4338)$ in the $B^- \to J/\psi\Lambda\bar{p}$ process[1] [49]. Obviously, the observed $P_{\psi s}^{\Lambda}(4459)$ and $P_{\psi s}^{\Lambda}(4338)$ not only make the family of the hidden-charm pentaquark with single strangeness becomes abundant, but also inspire theorist's interest in investigating the $\Xi_c\bar{D}^{(*)}$ molecular states [50–54].

In Ref. [52], we indicated the existence of characteristic spectrum of the $\Xi_c^{(\prime)}\bar{D}^{(*)}$-type hidden-charm molecular pentaquarks with single strangeness when checking the S-wave $\Xi_c^{(\prime)}\bar{D}^{(*)}$ interactions quantitatively. In fact, this behavior was also found by Karliner and Rosner in Ref. [51]. When facing such experimental and theoretical progresses of exploring the hidden-charm molecular pentaquarks with single strangeness, it is natural to expect that the theorists should pay more attention to exploring other properties of the S-wave isoscalar $\Xi_c^{(\prime)}\bar{D}^{(*)}$ molecular states, which is valuable to reveal the mystery behind these novel phenomena.

As is well known, the study of the electromagnetic properties of the hadrons can provide new insight to reveal their inner structures. For example, the magnetic moment

*wangfl2016@lzu.edu.cn
†zhouhy20@lzu.edu.cn
‡liuzhanwei@lzu.edu.cn
§xiangliu@lzu.edu.cn

[1]Since we are using the new LHCb exotic naming convention [49] for $P_{\psi s}^{\Lambda}(4338)$, the same label applies to $P_{cs}(4459)$, and that P_{ψ}^{N} would be the new name for the old P_c states.

of the $\Sigma_c\bar{D}^*$ molecular pentaquark with $I(J^P) = 1/2(1/2^-)$ is obviously different from that of the $\Sigma_c\bar{D}^*$ state with $I(J^P) = 1/2(3/2^-)$ [55,56]. This observation can be applied to clarify the spin-parity quantum numbers of the $P_\psi^N(4440)$ and $P_\psi^N(4457)$ [13–20]. In the past several decades, different theoretical methods or approaches were proposed to investigate the electromagnetic properties of the hadronic states [11]. Among them, the constituent quark model is a popular way to study the magnetic moments of the decuplet and octet baryons quantitatively [57,58].

Along this line, for further presenting the inner structures of the S-wave isoscalar $\Xi_c^{(\prime)}\bar{D}^{(*)}$ molecular states, it is essential to obtain the information of their magnetic moments, transition magnetic moments, and radiative decay behaviors, which will be the main task of this work. For achieving this goal, we adopt the constituent quark model in our realistic calculation since it has been adopted to investigate the magnetic moments of the hadronic molecular states [55,56,59–62]. In addition, the S-D wave mixing effect [52] is taken into account in our calculation. By this effort, we illustrate the electromagnetic properties of the S-wave isoscalar $\Xi_c^{(\prime)}\bar{D}^{(*)}$ molecular pentaquarks, and hope that the present work may inspire our colleagues to further focus on the electromagnetic properties of the S-wave isoscalar $\Xi_c^{(\prime)}\bar{D}^{(*)}$ molecules in the following years. In Ref. [63], the magnetic moments of the $P_{\psi s}^{\Lambda}(4338)$ and $P_{\psi s}^{\Lambda}(4459)$ states were obtained within the hadronic molecular picture by the QCD sum rule.

An outline of this paper is as follows. After Introduction, the detailed deduction of the magnetic moments and the transition magnetic moments related to the S-wave charmed baryons $\Xi_c^{(\prime)}$, the S-wave anticharmed mesons $\bar{D}^{(*)}$, and the S-wave isoscalar $\Xi_c^{(\prime)}\bar{D}^{(*)}$ molecular states will be given in Sec. II. With this preparation, we present the numerical results and the corresponding discussion of the magnetic moments, the transition magnetic moments, and the radiative decay behaviors of the S-wave isoscalar $\Xi_c^{(\prime)}\bar{D}^{(*)}$ molecular pentaquarks in Sec. III. Finally, this work ends with a short summary in Sec. IV.

II. DEDUCING THE ELECTROMAGNETIC PROPERTIES OF THE $\Xi_c^{(\prime)}\bar{D}^{(*)}$-TYPE MOLECULAR PENTAQUARKS

In this section, the main task is to deduce the magnetic moments and the transition magnetic moments of the S-wave charmed baryons $\Xi_c^{(\prime)}$, the S-wave anti-charmed mesons $\bar{D}^{(*)}$, and the S-wave isoscalar $\Xi_c^{(\prime)}\bar{D}^{(*)}$ molecular pentaquarks, where we adopt the constituent quark model in the calculation. We should emphasize that the constituent quark model was extensively applied to study various properties of the hadronic states in the past decades [2–12], where the magnetic moments of the hadronic molecular states were focused [55,56,59–62].

In the present work, the adopted model and convention of getting the hadronic magnetic moments and the transition magnetic moments are the same as those given in Refs. [56,62]. Within the constituent quark model, the magnetic moment of the hadronic state μ can be written as the sum of the spin magnetic moment $\mu_{\rm spin}$ and the orbital magnetic moment $\mu_{\rm orbital}$ from its constituents [55,59,62,64], i.e.,

$$\mu = \mu_{\rm spin} + \mu_{\rm orbital}. \tag{1}$$

Here, the spin magnetic moment $\mu_{\rm spin}$ and the orbital magnetic moment $\mu_{\rm orbital}$ can be related to the spin of each constituent and the orbital angular momenta between its constituents, respectively. Subsequently, we define the spin magnetic moment $\mu_{\rm spin}$ and the orbital magnetic moment $\mu_{\rm orbital}$ adopted in the present work.

In practice, the magnetic moment μ_{H_0} and the transition magnetic moment $\mu_{H_1\to H_2}$ can be calculated by the z-component of the magnetic moment operator $\hat{\mu}_z$ sandwiched by the corresponding wave functions of the investigated hadrons, and the general expression is

$$\mu_{H_0} = \langle H_0|\hat{\mu}_z|H_0\rangle, \tag{2}$$

$$\mu_{H_1\to H_2} = \langle H_2|\hat{\mu}_z|H_1\rangle, \tag{3}$$

where $|H_i\rangle$ stands for the corresponding wave function of the investigated hadronic state. Thus, the first task is to calculate the matrix elements $\langle H_0|\hat{\mu}_z|H_0\rangle$ and $\langle H_2|\hat{\mu}_z|H_1\rangle$ for extracting the hadronic magnetic moment and the transition magnetic moment.

The wave function of the hadronic state ψ is composed of the color wave function $\omega_{\rm color}$, the flavor wave function $\chi_{\rm flavor}$, the spin wave function $\chi_{\rm spin}$, and the spatial wave function $R_{\rm space}$, which can be factorized as

$$\psi = \omega_{\rm color} \otimes \chi_{\rm flavor} \otimes \chi_{\rm spin} \otimes R_{\rm space}. \tag{4}$$

For the hadronic wave function, we should emphasize:

(1) The color wave functions do not affect the magnetic moments of hadrons, and we do not need to consider them explicitly;
(2) For the flavor-spin wave function, we need to consider the requirement of the symmetry, which is an important step when getting the magnetic moment and the transition magnetic moment of the hadronic state;
(3) For the spatial wave function [62], we usually do not mention it when calculating the magnetic moment and the transition magnetic moment of the hadronic state. However, if considering the S-D wave mixing effect, we should take the spatial wave functions of

these involved mixing channels as input, which can be numerically obtained from solving the Schrödinger equation for the mass spectrum.

Due to the absence of experimental data of the magnetic moments and the transition magnetic moments of the S-wave charmed baryons $\Xi_c^{(\prime)}$ and the S-wave anti-charmed mesons $\bar{D}^{(*)}$, we first calculate them within the constituent quark model. For $\Xi_c^{(\prime)}$ and $\bar{D}^{(*)}$, there only exist the spin magnetic moments $\vec{\mu}_{\rm spin}$ since the orbital angular momentum among quarks is 0, and at quark level [55,59,62,64]

$$\vec{\mu}_{\rm spin} = \sum_i \frac{Q_i}{2M_i}\vec{\sigma}_i, \tag{5}$$

where Q_i, M_i, and $\vec{\sigma}_i$ denote the charge, mass, and Pauli's spin matrix of the ith quark, respectively.

In order to obtain the magnetic moments and the transition magnetic moments of $\Xi_c^{(\prime)}$ and $\overline{D}^{(*)}$, we need to construct their flavor wave functions and spin wave functions. Based on the flavor symmetries of the light diquark, the charmed baryons can be categorized into the $\bar{3}_F$ and 6_F flavor representations, which correspond to the flavor antisymmetry and symmetry for the light diquark, respectively. Here, Ξ_c with $J^P = 1/2^+$ denotes the S-wave charmed baryon in the $\bar{3}_F$ flavor representation, while Ξ_c' with $J^P = 1/2^+$ is for the 6_F flavor representation. In Table I, we collect these flavor wave functions $\chi_{\rm flavor}$ and the spin wave functions $\chi_{\rm spin}$ of $\Xi_c^{(\prime)}$ and $\bar{D}^{(*)}$ [65,66], which are adopted to calculate the matrix elements $\mu_{H_0} = \langle H_0|\hat{\mu}_z|H_0\rangle$ and $\mu_{H_1\to H_2} = \langle H_2|\hat{\mu}_z|H_1\rangle$.

TABLE I. The flavor wave functions $\chi_{\rm flavor}$ and the spin wave functions $\chi_{\rm spin}$ of the S-wave charmed baryons $\Xi_c^{(\prime)}$ and the S-wave anti-charmed mesons $\bar{D}^{(*)}$. Here, S and S_3 are the spin and its third component of the discussed hadron, while the arrow denotes the third component of the quark spin.

States	$\lvert S, S_3\rangle$	$\chi_{\rm flavor}\otimes\chi_{\rm spin}$
Ξ_c^+	$\lvert\frac{1}{2},\frac{1}{2}\rangle$	$\frac{1}{\sqrt{2}}(usc-suc)\otimes\frac{1}{\sqrt{2}}(\uparrow\downarrow\uparrow-\downarrow\uparrow\uparrow)$
	$\lvert\frac{1}{2},-\frac{1}{2}\rangle$	$\frac{1}{\sqrt{2}}(usc-suc)\otimes\frac{1}{\sqrt{2}}(\uparrow\downarrow\downarrow-\downarrow\uparrow\downarrow)$
Ξ_c^0	$\lvert\frac{1}{2},\frac{1}{2}\rangle$	$\frac{1}{\sqrt{2}}(dsc-sdc)\otimes\frac{1}{\sqrt{2}}(\uparrow\downarrow\uparrow-\downarrow\uparrow\uparrow)$
	$\lvert\frac{1}{2},-\frac{1}{2}\rangle$	$\frac{1}{\sqrt{2}}(dsc-sdc)\otimes\frac{1}{\sqrt{2}}(\uparrow\downarrow\downarrow-\downarrow\uparrow\downarrow)$
$\Xi_c'^+$	$\lvert\frac{1}{2},\frac{1}{2}\rangle$	$\frac{1}{\sqrt{2}}(usc+suc)\otimes\frac{1}{\sqrt{6}}(2\uparrow\uparrow\downarrow-\downarrow\uparrow\uparrow-\uparrow\downarrow\uparrow)$
	$\lvert\frac{1}{2},-\frac{1}{2}\rangle$	$\frac{1}{\sqrt{2}}(usc+suc)\otimes\frac{1}{\sqrt{6}}(\downarrow\uparrow\downarrow+\uparrow\downarrow\downarrow-2\downarrow\downarrow\uparrow)$
$\Xi_c'^0$	$\lvert\frac{1}{2},\frac{1}{2}\rangle$	$\frac{1}{\sqrt{2}}(dsc+sdc)\otimes\frac{1}{\sqrt{6}}(2\uparrow\uparrow\downarrow-\downarrow\uparrow\uparrow-\uparrow\downarrow\uparrow)$
	$\lvert\frac{1}{2},-\frac{1}{2}\rangle$	$\frac{1}{\sqrt{2}}(dsc+sdc)\otimes\frac{1}{\sqrt{6}}(\downarrow\uparrow\downarrow+\uparrow\downarrow\downarrow-2\downarrow\downarrow\uparrow)$
$\bar{D}^0$	$\lvert0,0\rangle$	$\bar{c}u\otimes\frac{1}{\sqrt{2}}(\uparrow\downarrow-\downarrow\uparrow)$
D^-	$\lvert0,0\rangle$	$\bar{c}d\otimes\frac{1}{\sqrt{2}}(\uparrow\downarrow-\downarrow\uparrow)$
$\bar{D}^{*0}$	$\lvert1,1\rangle$	$\bar{c}u\otimes\uparrow\uparrow$
	$\lvert1,0\rangle$	$\bar{c}u\otimes\frac{1}{\sqrt{2}}(\uparrow\downarrow+\downarrow\uparrow)$
	$\lvert1,-1\rangle$	$\bar{c}u\otimes\downarrow\downarrow$
D^{*-}	$\lvert1,1\rangle$	$\bar{c}d\otimes\uparrow\uparrow$
	$\lvert1,0\rangle$	$\bar{c}d\otimes\frac{1}{\sqrt{2}}(\uparrow\downarrow+\downarrow\uparrow)$
	$\lvert1,-1\rangle$	$\bar{c}d\otimes\downarrow\downarrow$

For these $\Xi_c^{(\prime)}$ and $\bar{D}^{(*)}$, their magnetic moments can be estimated by the z-component of the magnetic moment operator $\hat{\mu}_z$ sandwiched by the corresponding flavor-spin wave functions of $\Xi_c^{(\prime)}$ and $\bar{D}^{(*)}$, respectively. Here, we need to indicate that the magnetic moment of the quark can be obtained by the following matrix elements

$$\langle q\uparrow|\hat{\mu}_z|q\uparrow\rangle = \mu_q = \frac{Q_q}{2M_q}, \tag{6}$$

$$\langle q\downarrow|\hat{\mu}_z|q\downarrow\rangle = -\mu_q = -\frac{Q_q}{2M_q}. \tag{7}$$

Here, the arrow stands for the third component of the quark spin, while Q_q and M_q are the quark charge and mass, respectively. Additionally, we need to indicate that $\mu_{\bar{q}} = -\mu_q = -Q_q/2M_q$. For example,

$$\begin{aligned}\mu_{\bar{D}^{*0}} &= \langle\chi_{\bar{D}^{*0}}^{S=1;S_3=1}|\hat{\mu}_z|\chi_{\bar{D}^{*0}}^{S=1;S_3=1}\rangle \\ &= \langle\bar{c}u\uparrow\uparrow|\hat{\mu}_z|\bar{c}u\uparrow\uparrow\rangle \\ &= \mu_{\bar{c}} + \mu_u.\end{aligned} \tag{8}$$

Thus, the expression of the magnetic moment of the S-wave charmed meson $\bar{D}^{*0}$ is $\mu_{\bar{c}} + \mu_u$. In this work, we adopt the constituent quark masses $m_u = 0.336$ GeV, $m_d = 0.336$ GeV, $m_s = 0.450$ GeV, and $m_c = 1.680$ GeV [67] to present the hadronic magnetic moments and transition magnetic moments quantitatively, which are widely used to study the hadronic magnetic moments [56,62]. By numerical calculation, we can obtain the magnetic moment of $\bar{D}^{*0}$ is $1.489\mu_N$. Here, $\mu_N = e/2m_N$ is the nuclear magnetic moment with $m_N = 938$ MeV as the nuclear mass [66], which is the unit of the magnetic moment.

In Table II, we list the expressions and numerical results of the magnetic moments of $\Xi_c^{(\prime)}$ and $\bar{D}^{(*)}$, which are

TABLE II. The magnetic moments of the S-wave charmed baryons $\Xi_c^{(\prime)}$ and the S-wave anticharmed mesons $\bar{D}^{(*)}$. Here, the magnetic moments of the S-wave anti-charmed mesons $\bar{D}^0$ and D^- are zero, the magnetic moment is in unit of the nuclear magnetic moment μ_N, and $\mu_q = Q_q/2M_q$ with Q_q and M_q are the quark charge and mass, respectively.

Hadrons	Expressions	Results	Other works	
Ξ_c^+	μ_c	0.372	0.37 [67]	0.37 [68]
Ξ_c^0	μ_c	0.372	0.366 [67]	0.38 [69]
$\Xi_c'^+$	$\frac{2}{3}\mu_u+\frac{2}{3}\mu_s-\frac{1}{3}\mu_c$	0.654	0.65 [69]	0.633 [70]
$\Xi_c'^0$	$\frac{2}{3}\mu_d+\frac{2}{3}\mu_s-\frac{1}{3}\mu_c$	−1.208	−1.23 [71]	−1.23 [72]
$\bar{D}^{*0}$	$\mu_{\bar{c}}+\mu_u$	1.489	1.28 [70]	1.48 [73]
D^{*-}	$\mu_{\bar{c}}+\mu_d$	−1.303	−1.31 [73]	−1.17 [74]

expressed as the combination of the magnetic moments of their constituent quarks. In addition, we compare our obtained numerical results with those from other theoretical works, and we can see they are consistent [67–74]. Here, we need to emphasis that the magnetic moments of the S-wave anti-charmed mesons $\bar{D}^0$ and D^- are zero due to being spin 0. For example, the magnetic moment of $\bar{D}^0$ is explicitly written as

$$\begin{aligned}&\langle\chi^{S=0;S_3=0}_{\bar{D}^0}|\hat{\mu}_z|\chi^{S=0;S_3=0}_{\bar{D}^0}\rangle\\&=\left\langle\frac{\bar{c}u\uparrow\downarrow-\bar{c}u\downarrow\uparrow}{\sqrt{2}}\middle|\hat{\mu}_z\middle|\frac{\bar{c}u\uparrow\downarrow-\bar{c}u\downarrow\uparrow}{\sqrt{2}}\right\rangle\\&=0.\end{aligned}\tag{9}$$

Additionally, the transition magnetic moments of $\Xi_c^{(\prime)}$ and $\bar{D}^{(*)}$ can be obtained by calculating the matrix element $\mu_{H_1\to H_2}=\langle H_2|\hat{\mu}_z|H_1\rangle$, and the initial and final states take the same third components of the spin when deducing the hadronic transition magnetic moment. For instance,

$$\begin{aligned}\mu_{\bar{D}^{*0}\to\bar{D}^0}&=\langle\chi^{S=0;S_3=0}_{\bar{D}^0}|\hat{\mu}_z|\chi^{S=1;S_3=0}_{\bar{D}^{*0}}\rangle\\&=\left\langle\frac{\bar{c}u\uparrow\downarrow-\bar{c}u\downarrow\uparrow}{\sqrt{2}}\middle|\hat{\mu}_z\middle|\frac{\bar{c}u\uparrow\downarrow+\bar{c}u\downarrow\uparrow}{\sqrt{2}}\right\rangle\\&=\mu_{\bar{c}}-\mu_u.\end{aligned}\tag{10}$$

Thus, the expression and numerical result of the transition magnetic moment of the $\bar{D}^{*0}\to\bar{D}^0\gamma$ process are $\mu_{\bar{c}}-\mu_u$ and $-2.234\mu_N$, respectively.

In Table III, we present the expressions and numerical results of the transition magnetic moments of $\Xi_c^{(\prime)}$ and $\bar{D}^{(*)}$. In order to check the reliability of these obtained transition magnetic moments, we compare our obtained numerical results with those from other theoretical models, and our results are close to other theoretical predictions [67,70,73,75].

In our previous work [52], we already studied the S-wave $\Xi_c^{(\prime)}\bar{D}^{(*)}$-type mass spectrum of the hidden-charm molecular pentaquarks with strangeness, and our numerical results suggest that all of the S-wave isoscalar $\Xi_c^{(\prime)}\bar{D}^{(*)}$ states can be recommended as the hidden-charm molecular pentaquark candidates with strangeness. In this subsection, we mainly illustrate how to deduce the magnetic moments, the transition magnetic moments, and the radiative decay behaviors of these hidden-charm molecular pentaquark candidates with strangeness.

First we assume these molecular states are in S wave, and then we further take into account the S-D wave mixing effect. The S-wave hadronic state only has the spin magnetic moment $\mu_{\rm spin}$, and the D-wave hadronic state contains the spin magnetic moment $\mu_{\rm spin}$ and the orbital magnetic moment $\mu_{\rm orbital}$ from its constituents. Here, the orbital magnetic moments $\mu_{\rm orbital}$ of the D-wave $\Xi_c^{(\prime)}\bar{D}^{(*)}$ channels can be written as [55,56,59,62,64,76]

$$\begin{aligned}\vec{\mu}_{\rm orbital}&=\mu^L_{mb}\vec{L}\\&=\frac{M_m}{M_b+M_m}\frac{Q_b}{2M_b}\vec{L}+\frac{M_b}{M_b+M_m}\frac{Q_m}{2M_m}\vec{L},\end{aligned}\tag{11}$$

where the subscripts b and m correspond to the S-wave charmed baryons $\Xi_c^{(\prime)}$ and the S-wave anticharmed mesons $\bar{D}^{(*)}$, respectively, and $\vec{L}$ denotes the orbital angular momenta between $\Xi_c^{(\prime)}$ and $\bar{D}^{(*)}$. Here, we use the formula $\hat{L}_zY_{L,m_L}=m_LY_{L,m_L}$ and $\int Y^\dagger_{L,m_L}Y_{L,m_L}\sin\theta d\theta d\phi=1$ when deducing the hadronic orbital magnetic moments.

Similar to the magnetic moments and the transition magnetic moments of $\Xi_c^{(\prime)}$ and $\bar{D}^{(*)}$, the magnetic moments and the transition magnetic moments of the S-wave isoscalar $\Xi_c^{(\prime)}\bar{D}^{(*)}$ molecular states can be obtained by calculating the matrix elements $\mu_{H_0}=\langle H_0|\hat{\mu}_z|H_0\rangle$ and $\mu_{H_1\to H_2}=\langle H_2|\hat{\mu}_z|H_1\rangle$, respectively. In Table IV, we collect the flavor wave functions $\chi_{\rm flavor}$ and the spin wave functions

TABLE III. The transition magnetic moments of the S-wave charmed baryons $\Xi_c^{(\prime)}$ and the S-wave anticharmed mesons $\bar{D}^{(*)}$. Here, the transition magnetic moment is in unit of the nuclear magnetic moment μ_N.

Decay modes	Expressions	Results	Other works	
$\Xi_c^{\prime+}\to\Xi_c^+\gamma$	$\frac{1}{\sqrt{3}}(\mu_s-\mu_u)$	−1.476	−1.39 [67]	−1.4282 [75]
$\Xi_c^{\prime0}\to\Xi_c^0\gamma$	$\frac{1}{\sqrt{3}}(\mu_s-\mu_d)$	0.136	0.13 [67]	0.138 [70]
$\bar{D}^{*0}\to\bar{D}^0\gamma$	$\mu_{\bar{c}}-\mu_u$	−2.234	−2.13 [73]	
$D^{*-}\to D^-\gamma$	$\mu_{\bar{c}}-\mu_d$	0.558	0.54 [73]	

TABLE IV. The flavor wave functions $\chi_{\rm flavor}$ and the spin wave functions $\chi_{\rm spin}$ of the S-wave isoscalar $\Xi_c^{(\prime)}\bar{D}^{(*)}$ systems. Here, I and I_3 are the isospin and its third component of the investigated system, respectively, while S and S_3 are the spin and its third component of the investigated system, respectively.

Systems	$\lvert I,I_3\rangle$	$\chi_{\rm flavor}$
$\Xi_c^{(\prime)}\bar{D}^{(*)}$	$\lvert0,0\rangle$	$\frac{1}{\sqrt{2}}\lvert\Xi_c^{(\prime)+}D^{(*)-}\rangle-\frac{1}{\sqrt{2}}\lvert\Xi_c^{(\prime)0}\bar{D}^{(*)0}\rangle$
Systems	$\lvert S,S_3\rangle$	$\chi_{\rm spin}$
$\Xi_c^{(\prime)}\bar{D}$	$\lvert\frac{1}{2},\frac{1}{2}\rangle$	$\lvert\frac{1}{2},\frac{1}{2}\rangle\lvert0,0\rangle$
	$\lvert\frac{1}{2},-\frac{1}{2}\rangle$	$\lvert\frac{1}{2},-\frac{1}{2}\rangle\lvert0,0\rangle$
$\Xi_c^{(\prime)}\bar{D}^*$	$\lvert\frac{1}{2},\frac{1}{2}\rangle$	$\frac{1}{\sqrt{3}}\lvert\frac{1}{2},\frac{1}{2}\rangle\lvert1,0\rangle-\sqrt{\frac{2}{3}}\lvert\frac{1}{2},-\frac{1}{2}\rangle\lvert1,1\rangle$
	$\lvert\frac{1}{2},-\frac{1}{2}\rangle$	$\sqrt{\frac{2}{3}}\lvert\frac{1}{2},\frac{1}{2}\rangle\lvert1,-1\rangle-\frac{1}{\sqrt{3}}\lvert\frac{1}{2},-\frac{1}{2}\rangle\lvert1,0\rangle$
	$\lvert\frac{3}{2},\frac{3}{2}\rangle$	$\lvert\frac{1}{2},\frac{1}{2}\rangle\lvert1,1\rangle$
	$\lvert\frac{3}{2},\frac{1}{2}\rangle$	$\sqrt{\frac{2}{3}}\lvert\frac{1}{2},\frac{1}{2}\rangle\lvert1,0\rangle+\frac{1}{\sqrt{3}}\lvert\frac{1}{2},-\frac{1}{2}\rangle\lvert1,1\rangle$
	$\lvert\frac{3}{2},-\frac{1}{2}\rangle$	$\frac{1}{\sqrt{3}}\lvert\frac{1}{2},\frac{1}{2}\rangle\lvert1,-1\rangle+\sqrt{\frac{2}{3}}\lvert\frac{1}{2},-\frac{1}{2}\rangle\lvert1,0\rangle$
	$\lvert\frac{3}{2},-\frac{3}{2}\rangle$	$\lvert\frac{1}{2},-\frac{1}{2}\rangle\lvert1,-1\rangle$

$\chi_{\rm spin}$ for these discussed S-wave isoscalar $\Xi_c^{(\prime)}\bar{D}^{(*)}$ systems [52]. Now, we take $\mu_{\Xi_c\bar{D}|^2S_{1/2}\rangle}$ and $\mu_{\Xi_c'\bar{D}|^2S_{1/2}\rangle\to\Xi_c\bar{D}|^2S_{1/2}\rangle}$ as examples to illustrate the procedure of deducing the magnetic moments and the transition magnetic moments of the S-wave isoscalar $\Xi_c^{(\prime)}\bar{D}^{(*)}$ molecular states

$$\begin{aligned}\mu_{\Xi_c\bar{D}|^2S_{1/2}\rangle} &= \langle\chi_{\Xi_c\bar{D}|^2S_{1/2}\rangle}|\hat{\mu}_z|\chi_{\Xi_c\bar{D}|^2S_{1/2}\rangle}\rangle \\ &= \frac{1}{2}\mu_{\Xi_c^+} + \frac{1}{2}\mu_{\Xi_c^0}, \end{aligned} \tag{12}$$

$$\begin{aligned}\mu_{\Xi_c'\bar{D}|^2S_{1/2}\rangle\to\Xi_c\bar{D}|^2S_{1/2}\rangle} &= \langle\chi_{\Xi_c\bar{D}|^2S_{1/2}\rangle}|\hat{\mu}_z|\chi_{\Xi_c'\bar{D}|^2S_{1/2}\rangle}\rangle \\ &= \frac{1}{2}\mu_{\Xi_c'^+\to\Xi_c^+} + \frac{1}{2}\mu_{\Xi_c'^0\to\Xi_c^0}, \end{aligned} \tag{13}$$

respectively. Thus, we can obtain the magnetic moment of the $\Xi_c\bar{D}|^2S_{1/2}\rangle$ state and the transition magnetic moment of the $\Xi_c'\bar{D}|^2S_{1/2}\rangle\to\Xi_c\bar{D}|^2S_{1/2}\rangle\gamma$ process. Here, the notation $|^{2S+1}L_J\rangle$ is used. Additionally, S, L, and J denote the spin, orbit angular momentum, and total angular momentum quantum numbers for the discussed system, respectively.

After that, we further discuss the magnetic moments and the transition magnetic moments of the isoscalar $\Xi_c^{(\prime)}\bar{D}^{(*)}$ molecular states after considering the S-D wave mixing effect. Nevertheless, the isoscalar $\Xi_c^{(\prime)}\bar{D}$ states with $J^P = 1/2^-$ only exist the S-wave component, i.e., $|^2S_{1/2}\rangle$ channel, and the probabilities for the D-wave components are zero for the isoscalar $\Xi_c\bar{D}^*$ states with $J^P = 1/2^-$ and $J^P = 3/2^-$ [52]. In detail, since the contribution of the tensor forces from the $S-D$ wave mixing effect for the $\Xi_c\bar{D}^*$ interactions disappears, the probabilities for the D-wave components are zero for the isoscalar $\Xi_c\bar{D}^*$ states with $J^P = 1/2^-$ and $J^P = 3/2^-$ [52], and thus the contribution of the magnetic moment of the D-wave channel is zero. Thus for the S-D wave mixing effects we consider the following allowed channels [52], i.e.,

$$\begin{aligned}&\Xi_c'\bar{D}^*[J^P = 1/2^-]\colon |^2S_{1/2}\rangle, |^4D_{1/2}\rangle, \\ &\Xi_c'\bar{D}^*[J^P = 3/2^-]\colon |^4S_{3/2}\rangle, |^2D_{3/2}\rangle, |^4D_{3/2}\rangle.\end{aligned}$$

When considering the contribution of the S-D wave mixing effect, the hadronic magnetic moment can be written as $\sum_i \mu_i\langle R_i|R_i\rangle + \sum_{i\neq j}\mu_{i\to j}\langle R_j|R_i\rangle$, where R_i denotes the space wave function of the corresponding i-th channel, which can be obtained by the calculation of the mass spectrum. In the following, we take the S-wave isoscalar $\Xi_c'\bar{D}^*$ state with $J^P = 1/2^-$ as an example to illustrate how to obtain the hadronic magnetic moment after considering the S-D wave mixing effect. After performing the S-D wave mixing analysis, the specific expression of the magnetic moment of the S-wave isoscalar $\Xi_c'\bar{D}^*$ state with $J^P = 1/2^-$ can be written as

$$\begin{aligned}&\mu_{\Xi_c'\bar{D}^*|^2S_{1/2}\rangle}\langle R_{\Xi_c'\bar{D}^*|^2S_{1/2}\rangle}|R_{\Xi_c'\bar{D}^*|^2S_{1/2}\rangle}\rangle \\ &+ \mu_{\Xi_c'\bar{D}^*|^4D_{1/2}\rangle}\langle R_{\Xi_c'\bar{D}^*|^4D_{1/2}\rangle}|R_{\Xi_c'\bar{D}^*|^4D_{1/2}\rangle}\rangle. \end{aligned} \tag{14}$$

In the above expression, the $\mu_{\Xi_c\bar{D}^*|^2S_{1/2}\rangle}$ has been discussed in Eq. (12), and the involved components $\langle R_{\Xi_c'\bar{D}^*|^2S_{1/2}\rangle}|R_{\Xi_c'\bar{D}^*|^2S_{1/2}\rangle}\rangle$ and $\langle R_{\Xi_c'\bar{D}^*|^4D_{1/2}\rangle}|R_{\Xi_c'\bar{D}^*|^4D_{1/2}\rangle}\rangle$ can be obtained by solving the Schrödinger equation for the mass spectrum of the isoscalar $\Xi_c'\bar{D}^*$ state with $J^P = 1/2^-$ after considering the S-D wave mixing effect [52].

In the following, we illustrate the method of obtaining the magnetic moment of the $\Xi_c'\bar{D}^*|^4D_{1/2}\rangle$ channel. For these investigated hadronic states, their spin-orbit wave function can be constructed as

$$|^{2S+1}L_J\rangle = \sum_{m_S,m_L} C^{J,M}_{Sm_S,Lm_L}\chi_{S,m_S}Y_{L,m_L}. \tag{15}$$

Once expanding the spin-orbit wave function $|^4D_{1/2}\rangle$ for the $\Xi_c'\bar{D}^*$ system, we can obtain

$$\begin{aligned}|^4D_{1/2}\rangle &= \frac{1}{\sqrt{10}}\chi_{3/2,3/2}Y_{2,-1} - \frac{1}{\sqrt{5}}\chi_{3/2,1/2}Y_{2,0} \\ &+ \sqrt{\frac{3}{10}}\chi_{3/2,-1/2}Y_{2,1} - \sqrt{\frac{2}{5}}\chi_{3/2,-3/2}Y_{2,2}. \end{aligned} \tag{16}$$

With the above preparation, the magnetic moment of the $\Xi_c'\bar{D}^*|^4D_{1/2}\rangle$ channel can be deduced as

$$\begin{aligned}&\frac{1}{10}\left(\frac{1}{2}\mu_{\Xi_c'^+} + \frac{1}{2}\mu_{D^{*-}} + \frac{1}{2}\mu_{\Xi_c'^0} + \frac{1}{2}\mu_{\bar{D}^{*0}} - \mu^L_{\Xi_c'\bar{D}^*}\right) \\ &+ \frac{1}{5}\left(\frac{1}{6}\mu_{\Xi_c'^+} + \frac{1}{6}\mu_{D^{*-}} + \frac{1}{6}\mu_{\Xi_c'^0} + \frac{1}{6}\mu_{\bar{D}^{*0}}\right) \\ &+ \frac{3}{10}\left(-\frac{1}{6}\mu_{\Xi_c'^+} - \frac{1}{6}\mu_{D^{*-}} - \frac{1}{6}\mu_{\Xi_c'^0} - \frac{1}{6}\mu_{\bar{D}^{*0}} + \mu^L_{\Xi_c'\bar{D}^*}\right) \\ &+ \frac{2}{5}\left(-\frac{1}{2}\mu_{\Xi_c'^+} - \frac{1}{2}\mu_{D^{*-}} - \frac{1}{2}\mu_{\Xi_c'^0} - \frac{1}{2}\mu_{\bar{D}^{*0}} + 2\mu^L_{\Xi_c'\bar{D}^*}\right) \\ &= -\frac{1}{6}\mu_{\Xi_c'^+} - \frac{1}{6}\mu_{D^{*-}} - \frac{1}{6}\mu_{\Xi_c'^0} - \frac{1}{6}\mu_{\bar{D}^{*0}} + \mu^L_{\Xi_c'\bar{D}^*}. \end{aligned} \tag{17}$$

Through the above calculation, we can get the magnetic moment of the isoscalar $\Xi_c'\bar{D}^*$ state with $J^P = 1/2^-$ after considering the $S-D$ wave mixing effect.

In addition, the general expression of the hadronic transition magnetic moment can be written as $\sum_{i\neq j}\mu_{i\to j}\langle R_j|R_i\rangle$ when considering the contribution of the S-D wave mixing effect. Here, we need to mention that the calculation method of the transition magnetic moment is similar to that of the magnetic moment for the D-wave channel, except for the different wave functions of the initial and final states.

The radiative decay widths between the isoscalar $\Xi_c^{(\prime)}\bar{D}^{(*)}$ molecular states are the important physical observable in experiment, which may provide the crucial information to probe their inner structures. The radiative decay width is closely related to the transition magnetic moment. For the $H_1 \to H_2\gamma$ process, the photon momentum can be written as [70,75,77–79]

$$E_\gamma = \frac{M_1^2 - M_2^2}{2M_1}, \tag{18}$$

where H_1 and H_2 stand for these discussed hidden-charm molecular pentaquarks with strangeness, while M_1 and M_2 are the masses of the hadrons H_1 and H_2, respectively. The relation between the radiative decay width $\Gamma(H_1 \to H_2\gamma)$ and the transition magnetic moment $\mu_{H_1\to H_2}$ can be expressed as [70,75,77–79]

$$\Gamma(H_1 \to H_2\gamma) = \alpha_{\rm EM}\frac{E_\gamma^3}{M_P^2}\frac{2J_{H_2}+1}{2J_{H_1}+1}\left(\frac{\mu_{H_1\to H_2}}{\mu_N}\right)^2. \tag{19}$$

In the above formula, the fine structure constant is taken as $\alpha_{\rm EM} \approx 1/137$ and M_P is the proton mass with $M_P = 938$ MeV.

III. NUMERICAL ANALYSIS

In this section, we present the numerical results and discussions of the magnetic moments, the transition magnetic moments, and the radiative decay widths of the isoscalar $\Xi_c^{(\prime)}\bar{D}^{(*)}$ molecular states by performing the single channel analysis and the S-D wave mixing analysis, respectively. In Table V, the masses of these involved hadrons [66] are collected.

We first give the expressions and numerical results for the magnetic moments of the S-wave isoscalar hidden-charm $\Xi_c^{(\prime)}\bar{D}^{(*)}$ molecular states with strangeness in Table VI. To be more intuitive, we present their masses [33,46,52] and magnetic moments in Fig. 1.

Based on the obtained numerical results, we summarize the following points:

(i) Since the magnetic moment of $\bar{D}$ is zero, those of the S-wave isoscalar $\Xi_c^{(\prime)}\bar{D}$ molecules only contain the contribution from $\Xi_c^{(\prime)}$.

TABLE V. The summary of the masses of these involved hadrons [66].

Baryons	Masses (MeV)	Mesons	Masses (MeV)
Ξ_c^+	2467.71	D^-	1869.66
Ξ_c^0	2470.44	$\bar{D}^0$	1864.84
$\Xi_c^{\prime+}$	2578.20	D^{*-}	2010.26
$\Xi_c^{\prime 0}$	2578.70	$\bar{D}^{*0}$	2006.85

TABLE VI. The magnetic moments of the S-wave isoscalar $\Xi_c^{(\prime)}\bar{D}^{(*)}$-type hidden-charm molecular pentaquarks with strangeness obtained by performing the single channel analysis. Here, the magnetic moment is in unit of the nuclear magnetic moment μ_N.

States	$I(J^P)$	Expressions	Results
$\Xi_c\bar{D}$	$0(\frac{1}{2}^-)$	$\frac{1}{2}(\mu_{\Xi_c^+}+\mu_{\Xi_c^0})$	0.372
$\Xi_c'\bar{D}$	$0(\frac{1}{2}^-)$	$\frac{1}{2}(\mu_{\Xi_c'^+}+\mu_{\Xi_c'^0})$	−0.277
$\Xi_c\bar{D}^*$	$0(\frac{1}{2}^-)$	$-\frac{1}{6}(\mu_{\Xi_c^+}+\mu_{\Xi_c^0})+\frac{1}{3}(\mu_{D^{*-}}+\mu_{\bar{D}^{*0}})$	−0.062
	$0(\frac{3}{2}^-)$	$\frac{1}{2}(\mu_{\Xi_c^+}+\mu_{D^{*-}}+\mu_{\Xi_c^0}+\mu_{\bar{D}^{*0}})$	0.465
$\Xi_c'\bar{D}^*$	$0(\frac{1}{2}^-)$	$-\frac{1}{6}(\mu_{\Xi_c'^+}+\mu_{\Xi_c'^0})+\frac{1}{3}(\mu_{D^{*-}}+\mu_{\bar{D}^{*0}})$	0.154
	$0(\frac{3}{2}^-)$	$\frac{1}{2}(\mu_{\Xi_c'^+}+\mu_{D^{*-}}+\mu_{\Xi_c'^0}+\mu_{\bar{D}^{*0}})$	−0.184

(ii) The magnetic moment of the S-wave isoscalar $\Xi_c\bar{D}^*$ molecule with $J^P = 1/2^-$ is $-0.062\mu_N$, while those with $J^P = 3/2^-$ is $0.465\mu_N$. Thus, they are much different, which deserves to attract the attentions in the future experiments.

(iii) Similar to the $\Xi_c\bar{D}^*$ case, the magnetic moment of the S-wave isoscalar $\Xi_c'\bar{D}^*$ molecule with $J^P = 1/2^-$ is obviously different from that with $J^P = 3/2^-$. If the magnetic moment sign is measured as positive in the future experiments, the spin-parity quantum number of the S-wave isoscalar $\Xi_c'\bar{D}^*$ molecular state would be $J^P = 1/2^-$ rather than $J^P = 3/2^-$.

(iv) The S-wave isoscalar $\Xi_c\bar{D}^{(*)}$ and $\Xi_c'\bar{D}^{(*)}$ states with the same spin-parity quantum numbers have same spin wave functions (see Table IV for more details), but their magnetic moments are different, which is because the magnetic moment of Ξ_c is significantly different from that of Ξ_c'. Therefore, studying the magnetic moments can provide useful hints to probe the inner structures of these isoscalar $\Xi_c^{(\prime)}\bar{D}^{(*)}$ molecular states.

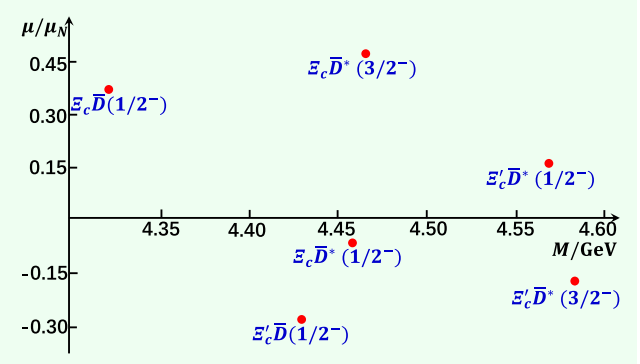

FIG. 1. The masses and magnetic moments of the S-wave isoscalar $\Xi_c^{(\prime)}\bar{D}^{(*)}$ molecular states. Here, we estimate the mass positions of these hidden-charm molecular pentaquarks with strangeness based on the results from Refs. [33,46,52].

Through the above analysis, we can conclude that the discussion of the magnetic moments can provide crucial information to understand their inner structures. To some extent, this fact shows the importance of exploring the hadronic magnetic moments, and we wish that more experimental and theoretical colleagues pay more attention to discussing the magnetic moment properties of the S-wave isoscalar $\Xi_c^{(\prime)}\bar{D}^{(*)}$ molecular states in the near future.

And then, we discuss the transition magnetic moments and the corresponding radiative decay widths between the S-wave isoscalar $\Xi_c^{(\prime)}\bar{D}^{(*)}$ molecular states, which include:

$$\begin{aligned}
&\Xi_c'\bar{D}|1/2^-\rangle \to \Xi_c\bar{D}|1/2^-\rangle\gamma,\\
&\Xi_c\bar{D}^*|1/2^-\rangle \to \Xi_c\bar{D}|1/2^-\rangle\gamma,\\
&\Xi_c\bar{D}^*|3/2^-\rangle \to \Xi_c\bar{D}|1/2^-\rangle\gamma,\\
&\Xi_c'\bar{D}^*|1/2^-\rangle \to \Xi_c\bar{D}|1/2^-\rangle\gamma,\\
&\Xi_c'\bar{D}^*|3/2^-\rangle \to \Xi_c\bar{D}|1/2^-\rangle\gamma,\\
&\Xi_c\bar{D}^*|1/2^-\rangle \to \Xi_c'\bar{D}|1/2^-\rangle\gamma,\\
&\Xi_c\bar{D}^*|3/2^-\rangle \to \Xi_c'\bar{D}|1/2^-\rangle\gamma,\\
&\Xi_c'\bar{D}^*|1/2^-\rangle \to \Xi_c'\bar{D}|1/2^-\rangle\gamma,\\
&\Xi_c'\bar{D}^*|3/2^-\rangle \to \Xi_c'\bar{D}|1/2^-\rangle\gamma,\\
&\Xi_c\bar{D}^*|3/2^-\rangle \to \Xi_c\bar{D}^*|1/2^-\rangle\gamma,\\
&\Xi_c'\bar{D}^*|1/2^-\rangle \to \Xi_c\bar{D}^*|1/2^-\rangle\gamma,\\
&\Xi_c'\bar{D}^*|3/2^-\rangle \to \Xi_c\bar{D}^*|1/2^-\rangle\gamma,\\
&\Xi_c'\bar{D}^*|1/2^-\rangle \to \Xi_c\bar{D}^*|3/2^-\rangle\gamma,\\
&\Xi_c'\bar{D}^*|3/2^-\rangle \to \Xi_c\bar{D}^*|3/2^-\rangle\gamma,\\
&\Xi_c'\bar{D}^*|3/2^-\rangle \to \Xi_c'\bar{D}^*|1/2^-\rangle\gamma.
\end{aligned}$$

Similar to the magnetic moments of the S-wave isoscalar $\Xi_c^{(\prime)}\bar{D}^*$ molecular states, we expect that the study of the transition magnetic moments and the radiative decay behaviors can provide important hints to disclose their inner structures.

In Table VII, we present the expressions and numerical results of the transition magnetic moments between the S-wave isoscalar $\Xi_c^{(\prime)}\bar{D}^{(*)}$-type hidden-charm molecular pentaquarks with strangeness. Among them, the largest and smallest transition magnetic moments correspond to the $\Xi_c\bar{D}^*|3/2^-\rangle \to \Xi_c\bar{D}^*|1/2^-\rangle\gamma$ and the $\Xi_c^{(\prime)}\bar{D}^*|3/2^-\rangle \to \Xi_c^{(\prime)}\bar{D}|1/2^-\rangle\gamma$ processes, respectively.

By performing numerical calculation, we can find that the transition magnetic moments between the S-wave isoscalar $\Xi_c^{(\prime)}\bar{D}^{(*)}$ molecular states exist following important relations, i.e.,

$$\begin{aligned}
\frac{\mu_{\Xi_c\bar{D}^*|\frac{1}{2}^-\rangle\to\Xi_c\bar{D}|\frac{1}{2}^-\rangle}}{\mu_{\Xi_c\bar{D}^*|\frac{3}{2}^-\rangle\to\Xi_c\bar{D}|\frac{1}{2}^-\rangle}} &= \frac{1}{\sqrt{2}},\\
\frac{\mu_{\Xi_c'\bar{D}^*|\frac{1}{2}^-\rangle\to\Xi_c'\bar{D}|\frac{1}{2}^-\rangle}}{\mu_{\Xi_c'\bar{D}^*|\frac{3}{2}^-\rangle\to\Xi_c'\bar{D}|\frac{1}{2}^-\rangle}} &= \frac{1}{\sqrt{2}},\\
\frac{\mu_{\Xi_c'\bar{D}^*|\frac{1}{2}^-\rangle\to\Xi_c\bar{D}^*|\frac{1}{2}^-\rangle}}{\mu_{\Xi_c'\bar{D}^*|\frac{3}{2}^-\rangle\to\Xi_c\bar{D}^*|\frac{1}{2}^-\rangle}} &= -\frac{1}{2\sqrt{2}},\\
\frac{\mu_{\Xi_c'\bar{D}^*|\frac{1}{2}^-\rangle\to\Xi_c\bar{D}^*|\frac{3}{2}^-\rangle}}{\mu_{\Xi_c'\bar{D}^*|\frac{3}{2}^-\rangle\to\Xi_c\bar{D}^*|\frac{3}{2}^-\rangle}} &= \frac{2\sqrt{2}}{3},
\end{aligned} \tag{20}$$

which are determined by the flavor-spin wave functions of the initial and final states. From Eq. (20), we can see that there are differences between the transition magnetic moments of the S-wave isoscalar $\Xi_c^{(\prime)}\bar{D}^*$ molecules with $J^P = 1/2^-$ and $J^P = 3/2^-$.

TABLE VII. The transition magnetic moments between the S-wave isoscalar $\Xi_c^{(\prime)}\bar{D}^{(*)}$-type hidden-charm molecular pentaquarks with strangeness obtained by performing the single channel analysis. Here, the magnetic moment is in unit of the nuclear magnetic moment μ_N.

Decay modes	Expressions	Results
$\Xi_c'\bar{D}\|\frac{1}{2}^-\rangle \to \Xi_c\bar{D}\|\frac{1}{2}^-\rangle\gamma$	$\frac{1}{2}(\mu_{\Xi_c'^+\to\Xi_c^+}+\mu_{\Xi_c'^0\to\Xi_c^0})$	−0.670
$\Xi_c\bar{D}^*\|\frac{1}{2}^-\rangle \to \Xi_c\bar{D}\|\frac{1}{2}^-\rangle\gamma$	$\frac{1}{2\sqrt{3}}(\mu_{D^{*-}\to D^-}+\mu_{\bar{D}^{*0}\to\bar{D}^0})$	−0.484
$\Xi_c\bar{D}^*\|\frac{3}{2}^-\rangle \to \Xi_c\bar{D}\|\frac{1}{2}^-\rangle\gamma$	$\frac{1}{\sqrt{6}}(\mu_{D^{*-}\to D^-}+\mu_{\bar{D}^{*0}\to\bar{D}^0})$	−0.684
$\Xi_c'\bar{D}^*\|\frac{1}{2}^-\rangle \to \Xi_c'\bar{D}\|\frac{1}{2}^-\rangle\gamma$	$\frac{1}{2\sqrt{3}}(\mu_{D^{*-}\to D^-}+\mu_{\bar{D}^{*0}\to\bar{D}^0})$	−0.484
$\Xi_c'\bar{D}^*\|\frac{3}{2}^-\rangle \to \Xi_c'\bar{D}\|\frac{1}{2}^-\rangle\gamma$	$\frac{1}{\sqrt{6}}(\mu_{D^{*-}\to D^-}+\mu_{\bar{D}^{*0}\to\bar{D}^0})$	−0.684
$\Xi_c\bar{D}^*\|\frac{3}{2}^-\rangle \to \Xi_c\bar{D}^*\|\frac{1}{2}^-\rangle\gamma$	$\frac{\sqrt{2}}{3}(\mu_{\Xi_c^+}+\mu_{\Xi_c^0})-\frac{1}{3\sqrt{2}}(\mu_{D^{*-}}+\mu_{\bar{D}^{*0}})$	0.307
$\Xi_c'\bar{D}^*\|\frac{1}{2}^-\rangle \to \Xi_c\bar{D}^*\|\frac{1}{2}^-\rangle\gamma$	$-\frac{1}{6}(\mu_{\Xi_c'^+\to\Xi_c^+}+\mu_{\Xi_c'^0\to\Xi_c^0})$	0.223
$\Xi_c'\bar{D}^*\|\frac{3}{2}^-\rangle \to \Xi_c\bar{D}^*\|\frac{1}{2}^-\rangle\gamma$	$\frac{\sqrt{2}}{3}(\mu_{\Xi_c'^+\to\Xi_c^+}+\mu_{\Xi_c'^0\to\Xi_c^0})$	−0.632
$\Xi_c'\bar{D}^*\|\frac{1}{2}^-\rangle \to \Xi_c\bar{D}^*\|\frac{3}{2}^-\rangle\gamma$	$\frac{\sqrt{2}}{3}(\mu_{\Xi_c'^+\to\Xi_c^+}+\mu_{\Xi_c'^0\to\Xi_c^0})$	−0.632
$\Xi_c'\bar{D}^*\|\frac{3}{2}^-\rangle \to \Xi_c\bar{D}^*\|\frac{3}{2}^-\rangle\gamma$	$\frac{1}{2}(\mu_{\Xi_c'^+\to\Xi_c^+}+\mu_{\Xi_c'^0\to\Xi_c^0})$	−0.670
$\Xi_c'\bar{D}^*\|\frac{3}{2}^-\rangle \to \Xi_c'\bar{D}^*\|\frac{1}{2}^-\rangle\gamma$	$\frac{\sqrt{2}}{3}(\mu_{\Xi_c'^+}+\mu_{\Xi_c'^0})-\frac{1}{3\sqrt{2}}(\mu_{D^{*-}}+\mu_{\bar{D}^{*0}})$	−0.305

More interestingly, the transition magnetic moments between the S-wave isoscalar $\Xi_c^{(\prime)}\bar{D}^{(*)}$ molecular states exist several equality relations, such as

$$\begin{aligned}
\frac{\mu_{\Xi_c'\bar{D}|\frac{1}{2}^-\rangle\to\Xi_c\bar{D}|\frac{1}{2}^-\rangle}}{\mu_{\Xi_c'\bar{D}^*|\frac{3}{2}^-\rangle\to\Xi_c\bar{D}^*|\frac{3}{2}^-\rangle}} &= 1,\\
\frac{\mu_{\Xi_c\bar{D}^*|\frac{1}{2}^-\rangle\to\Xi_c\bar{D}|\frac{1}{2}^-\rangle}}{\mu_{\Xi_c'\bar{D}^*|\frac{1}{2}^-\rangle\to\Xi_c'\bar{D}|\frac{1}{2}^-\rangle}} &= 1,\\
\frac{\mu_{\Xi_c\bar{D}^*|\frac{3}{2}^-\rangle\to\Xi_c\bar{D}|\frac{1}{2}^-\rangle}}{\mu_{\Xi_c'\bar{D}^*|\frac{3}{2}^-\rangle\to\Xi_c'\bar{D}|\frac{1}{2}^-\rangle}} &= 1,\\
\frac{\mu_{\Xi_c'\bar{D}^*|\frac{3}{2}^-\rangle\to\Xi_c\bar{D}^*|\frac{1}{2}^-\rangle}}{\mu_{\Xi_c'\bar{D}^*|\frac{1}{2}^-\rangle\to\Xi_c\bar{D}^*|\frac{3}{2}^-\rangle}} &= 1. \qquad (21)
\end{aligned}$$

Therefore, we hope that such qualitative relations of Eqs. (20)–(21) can be further tested in the future experiments and other theoretical approaches, which also can be regarded as important relations to check our theoretical predictions.

After getting the transition magnetic moments between the S-wave isoscalar $\Xi_c^{(\prime)}\bar{D}^{(*)}$ molecular states, we further discuss the radiative decay behaviors between the S-wave isoscalar $\Xi_c^{(\prime)}\bar{D}^{(*)}$ molecular states. As illustrated in Eqs. (18)–(19), the radiative decay widths depend on the binding energies of the initial and final molecules. For simplicity, we adopt the same binding energies for the initial and final molecules and take -1.0 MeV, -6.0 MeV, and -12.0 MeV to discuss the radiative decay widths between the S-wave isoscalar $\Xi_c^{(\prime)}\bar{D}^{(*)}$ molecular states in the absence of experimental data, which is similar to present the bound properties of the S-wave isoscalar $\Xi_c^{(\prime)}\bar{D}^{(*)}$ states in Ref. [52]. In Table VIII, we show the numerical results of the radiative decay widths between the S-wave isoscalar $\Xi_c^{(\prime)}\bar{D}^{(*)}$-type hidden-charm molecular pentaquarks with strangeness.

For these obtained radiative decay widths between the S-wave isoscalar $\Xi_c^{(\prime)}\bar{D}^{(*)}$ molecules, we need to point out that the binding energies of the S-wave isoscalar $\Xi_c^{(\prime)}\bar{D}^{(*)}$ moleculur states are very small compared with their mass thresholds, which can explain why the binding energies of the S-wave isoscalar $\Xi_c^{(\prime)}\bar{D}^{(*)}$ molecules play a minor role for their radiative decay widths [62]. Furthermore, most of the radiative decay widths between the S-wave isoscalar $\Xi_c^{(\prime)}\bar{D}^{(*)}$ molecular states are around 5.0 keV, while the decay width of the $\Xi_c'\bar{D}^*|1/2^-\rangle\to\Xi_c\bar{D}^*|1/2^-\rangle\gamma$ process is less than 1.0 keV, which is because the transition magnetic moment is small in this process.

When taking same binding energies for the S-wave isoscalar $\Xi_c\bar{D}^*$ molecular states with $J^P=1/2^-$ and $J^P=3/2^-$, we find that there exist same radiative decay widths for the $\Xi_c\bar{D}^*|1/2^-\rangle\to\Xi_c\bar{D}|1/2^-\rangle\gamma$ and $\Xi_c\bar{D}^*|3/2^-\rangle\to\Xi_c\bar{D}|1/2^-\rangle\gamma$ processes, since both radiative decay processes have the same $\mu^2_{H_1\to H_2}/(2J+1)$. As stressed in Ref. [52], the binding energies of the S-wave isoscalar $\Xi_c\bar{D}^*$ molecular states with $J^P=1/2^-$ and $J^P=3/2^-$ can be different slightly, which may result in the small difference of the radiative decay widths for the $\Xi_c\bar{D}^*|1/2^-\rangle\to\Xi_c\bar{D}|1/2^-\rangle\gamma$ and $\Xi_c\bar{D}^*|3/2^-\rangle\to\Xi_c\bar{D}|1/2^-\rangle\gamma$ processes. Here, we need to mention that the $P^{\Lambda}_{\psi s}(4459)$ existing in the $J/\psi\Lambda$ invariant mass spectrum may be described by two peak structures, and the corresponding masses are around 4454.9 MeV and 4467.9 MeV, respectively [21]. If the masses of the S-wave isoscalar $\Xi_c\bar{D}^*$ molecular states with $J^P=1/2^-$ and $J^P=3/2^-$ are 4454.9 MeV and 4467.9 MeV, we can estimate

$$\begin{aligned}
\Gamma(\Xi_c\bar{D}^*|1/2^-\rangle\to\Xi_c\bar{D}|1/2^-\rangle\gamma) &= 3.596\ \text{keV},\\
\Gamma(\Xi_c\bar{D}^*|3/2^-\rangle\to\Xi_c\bar{D}|1/2^-\rangle\gamma) &= 4.813\ \text{keV},
\end{aligned}$$

respectively. Meanwhile, it is interesting to note that the radiative decay behaviors of the $\Xi_c'\bar{D}^*|1/2^-\rangle\to\Xi_c\bar{D}|1/2^-\rangle\gamma$ and $\Xi_c'\bar{D}^*|3/2^-\rangle\to\Xi_c\bar{D}|1/2^-\rangle\gamma$ processes are similar to that of the $\Xi_c\bar{D}^*|1/2^-\rangle\to\Xi_c\bar{D}|1/2^-\rangle\gamma$ and $\Xi_c\bar{D}^*|3/2^-\rangle\to\Xi_c\bar{D}|1/2^-\rangle\gamma$ processes, which is due to the similarity between the S-wave isoscalar $\Xi_c\bar{D}^{(*)}$ states and the S-wave isoscalar $\Xi_c'\bar{D}^{(*)}$ states.

In addition, when adopting same binding energies for the S-wave isoscalar $\Xi_c^{(\prime)}\bar{D}^*$ molecular states with $J^P=1/2^-$ and $J^P=3/2^-$, it is obvious that the radiative decay widths are zero for the $\Xi_c\bar{D}^*|3/2^-\rangle\to\Xi_c\bar{D}^*|1/2^-\rangle\gamma$ and $\Xi_c'\bar{D}^*|3/2^-\rangle\to\Xi_c'\bar{D}^*|1/2^-\rangle\gamma$ processes. In practice, the binding energies of the S-wave isoscalar $\Xi_c^{(\prime)}\bar{D}^*$ molecular states with $J^P=1/2^-$ and $J^P=3/2^-$ can exist difference [52]. Here, we present the dependence of the radiative decay width of the $\Xi_c\bar{D}^*|3/2^-\rangle\to\Xi_c\bar{D}^*|1/2^-\rangle\gamma$ process on the binding energies of the $\Xi_c\bar{D}^*$ molecule with $I(J^P)=0(1/2^-)$ and $I(J^P)=0(3/2^-)$ in Fig. 2. In addition, we

TABLE VIII. The radiative decay widths between the S-wave isoscalar $\Xi_c^{(\prime)}\bar{D}^{(*)}$-type hidden-charm molecular pentaquarks with strangeness obtained by performing the single channel analysis. Here, the radiative decay width is in units of keV.

Decay modes	-1.0 MeV	-6.0 MeV	-12.0 MeV
$\Xi_c'\bar{D}\|\frac{1}{2}^-\rangle\to\Xi_c\bar{D}\|\frac{1}{2}^-\rangle\gamma$	4.710	4.694	4.675
$\Xi_c\bar{D}^*\|\frac{1}{2}^-\rangle\to\Xi_c\bar{D}\|\frac{1}{2}^-\rangle\gamma$	5.239	5.221	5.200
$\Xi_c\bar{D}^*\|\frac{3}{2}^-\rangle\to\Xi_c\bar{D}\|\frac{1}{2}^-\rangle\gamma$	5.239	5.221	5.200
$\Xi_c'\bar{D}^*\|\frac{1}{2}^-\rangle\to\Xi_c'\bar{D}\|\frac{1}{2}^-\rangle\gamma$	5.244	5.227	5.206
$\Xi_c'\bar{D}^*\|\frac{3}{2}^-\rangle\to\Xi_c'\bar{D}\|\frac{1}{2}^-\rangle\gamma$	5.244	5.227	5.206
$\Xi_c'\bar{D}^*\|\frac{1}{2}^-\rangle\to\Xi_c\bar{D}^*\|\frac{1}{2}^-\rangle\gamma$	0.524	0.522	0.520
$\Xi_c'\bar{D}^*\|\frac{3}{2}^-\rangle\to\Xi_c\bar{D}^*\|\frac{1}{2}^-\rangle\gamma$	2.096	2.089	2.080
$\Xi_c'\bar{D}^*\|\frac{1}{2}^-\rangle\to\Xi_c\bar{D}^*\|\frac{3}{2}^-\rangle\gamma$	8.382	8.354	8.322
$\Xi_c'\bar{D}^*\|\frac{3}{2}^-\rangle\to\Xi_c\bar{D}^*\|\frac{3}{2}^-\rangle\gamma$	4.714	4.700	4.680

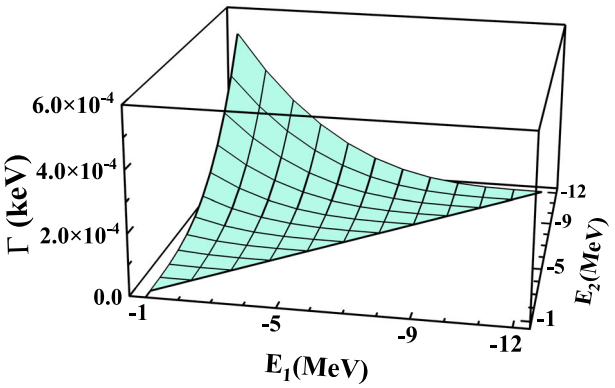

FIG. 2. The dependence of the radiative decay width Γ of the $\Xi_c\bar{D}^*|3/2^-\rangle \to \Xi_c\bar{D}^*|1/2^-\rangle\gamma$ process on the binding energy E_1 of the $\Xi_c\bar{D}^*$ molecule with $I(J^P) = 0(1/2^-)$ and the binding energy E_2 of the $\Xi_c\bar{D}^*$ molecule with $I(J^P) = 0(3/2^-)$. Here, the transition magnetic moment of the $\Xi_c\bar{D}^*|3/2^-\rangle \to \Xi_c\bar{D}^*|1/2^-\rangle\gamma$ process is taken as $0.307\mu_N$.

show the dependence of the radiative decay width of the $\Xi_c'\bar{D}^*|3/2^-\rangle \to \Xi_c'\bar{D}^*|1/2^-\rangle\gamma$ process on the binding energies of the $\Xi_c'\bar{D}^*$ molecule with $I(J^P) = 0(1/2^-)$ and $I(J^P) = 0(3/2^-)$ in Fig. 3. According to our quantitative calculation, the radiative decay widths of the $\Xi_c\bar{D}^*|3/2^-\rangle \to \Xi_c\bar{D}^*|1/2^-\rangle\gamma$ and $\Xi_c'\bar{D}^*|3/2^-\rangle \to \Xi_c'\bar{D}^*|1/2^-\rangle\gamma$ processes are less than 0.001 keV. The main reason is that the hadronic molecule is a loosely bound state with the reasonable binding energy at most tens of MeV [5], and the masses of the S-wave isoscalar $\Xi_c^{(\prime)}\bar{D}^*$ states with $J^P = 1/2^-$ and $J^P = 3/2^-$ are extremely close to each other in the hadronic molecular picture [52], which leads to the suppression of the kinetic phase space for both radiative decay processes. Furthermore, if the masses of the S-wave isoscalar $\Xi_c\bar{D}^*$ molecular states with $J^P = 1/2^-$ and $J^P = 3/2^-$ are taken as 4454.9 MeV and 4467.9 MeV [21], the radiative decay width of the

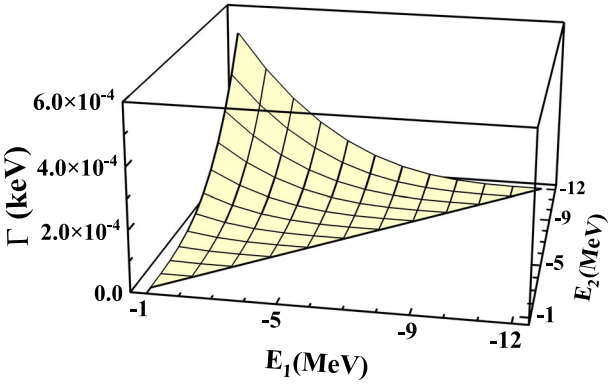

FIG. 3. The dependence of the radiative decay width Γ of the $\Xi_c'\bar{D}^*|3/2^-\rangle \to \Xi_c'\bar{D}^*|1/2^-\rangle\gamma$ process on the binding energy E_1 of the $\Xi_c'\bar{D}^*$ molecule with $I(J^P) = 0(1/2^-)$ and the binding energy E_2 of the $\Xi_c'\bar{D}^*$ molecule with $I(J^P) = 0(3/2^-)$. Here, the transition magnetic moment of the $\Xi_c'\bar{D}^*|3/2^-\rangle \to \Xi_c'\bar{D}^*|1/2^-\rangle\gamma$ process is taken as $-0.305\mu_N$.

$\Xi_c\bar{D}^*|3/2^-\rangle \to \Xi_c\bar{D}^*|1/2^-\rangle\gamma$ process is predicted to be around 0.0008 keV.

In the above discussion, we mainly focus on the magnetic moments, the transition magnetic moments, and the radiative decay behaviors of the S-wave isoscalar $\Xi_c^{(\prime)}\bar{D}^{(*)}$ molecular states by performing the single channel analysis, which provides valuable information to reflect their inner structures. Next, we further discuss them with considering the S-D wave mixing effect. According to our previous results on the mass spectrum [52], we find that the S-wave channels have the dominant contribution with the probabilities over 95 percent and play a major role for the isoscalar $\Xi_c'\bar{D}^*$ molecular states with $J^P = 1/2^-$ and $J^P = 3/2^-$. Thus, we naturally conjecture that the D-wave components with small contributions do not obviously decorate the magnetic moments of the S-wave isoscalar $\Xi_c'\bar{D}^*$ molecular states with $J^P = 1/2^-$ and $J^P = 3/2^-$ and the transition magnetic moment of the $\Xi_c'\bar{D}^*|3/2^-\rangle \to \Xi_c'\bar{D}^*|1/2^-\rangle\gamma$ process. Indeed, our following numerical results support such conjecture.

Due to the lack of the experimental data for the binding energies of the S-wave isoscalar $\Xi_c'\bar{D}^*$ molecules with $J^P = 1/2^-$ and $J^P = 3/2^-$, while the hadronic molecule is a loosely bound state [5], we discuss their magnetic moments by varying the binding energies of the S-wave isoscalar $\Xi_c'\bar{D}^*$ molecular states with $J^P = 1/2^-$ and $J^P = 3/2^-$ in the range of $-1 \sim -12$ MeV [52]. In Fig. 4, we present the magnetic moment dependence of the binding energies for the isoscalar $\Xi_c'\bar{D}^*$ molecular states with $J^P = 1/2^-$ and $J^P = 3/2^-$ by performing the S-D wave mixing analysis.

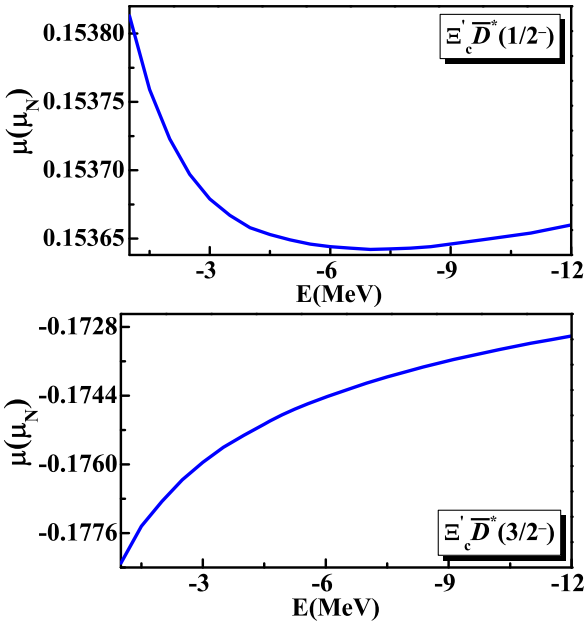

FIG. 4. The magnetic moments dependent on the binding energies for the isoscalar $\Xi_c'\bar{D}^*$ molecules with $J^P = 1/2^-$ and $J^P = 3/2^-$ after considering the S-D wave mixing effect.

After including the contribution of the D-wave channels, we can find that the magnetic moments of the isoscalar $\Xi_c'\bar{D}^*$ molecular states with $J^P = 1/2^-$ and $J^P = 3/2^-$ are $0.1538\ \mu_N \sim 0.1536\ \mu_N$ and $-0.1783\ \mu_N \sim -0.1730\ \mu_N$ with the binding energies of the corresponding systems in the range from -1 to -12 MeV, respectively. Furthermore, their magnetic moments are not obviously dependent on the binding energies of the S-wave isoscalar $\Xi_c'\bar{D}^*$ molecules with $J^P = 1/2^-$ and $J^P = 3/2^-$. By comparing the numerical results for the single channel case, it is obvious that the $S-D$ wave mixing effect plays a rather minor role, and the change of their magnetic moments is less than $0.02\mu_N$ when adding the contribution of the D-wave channels since the components of the D-wave channels are very tiny [52].

Following the procedure discussed above, we also study the transition magnetic moment of the $\Xi_c'\bar{D}^*|3/2^-\rangle \to \Xi_c'\bar{D}^*|1/2^-\rangle\gamma$ process by considering the S-D wave mixing effect, and the relevant numerical result is given in Fig. 5. Here, we discuss the transition magnetic moment of the $\Xi_c'\bar{D}^*|3/2^-\rangle \to \Xi_c'\bar{D}^*|1/2^-\rangle\gamma$ process by scanning the binding energies of the S-wave isoscalar $\Xi_c'\bar{D}^*$ molecular states with $J^P = (1/2^-, 3/2^-)$ in the range of $-1 \sim -12$ MeV.

As presented in Fig. 5, the transition magnetic moment of the $\Xi_c'\bar{D}^*|3/2^-\rangle \to \Xi_c'\bar{D}^*|1/2^-\rangle\gamma$ process is $-0.298\ \mu_N \sim -0.289\ \mu_N$ by tuning the binding energies of the corresponding discussed systems from -1 MeV to -12 MeV, which is slightly bigger than the numerical result $-0.305\ \mu_N$ from the single channel analysis. On the other hand, it shows that the radiative decay width of the $\Xi_c'\bar{D}^*|3/2^-\rangle \to \Xi_c'\bar{D}^*|1/2^-\rangle\gamma$ process becomes smaller when adding the contribution of the D-wave channels.

In the present experiments, there are difficulties in identifying the low-energy photons, which is a big challenge to distinguish the spin-parity quantum numbers of the isoscalar $\Xi_c^{(\prime)}\bar{D}^*$ molecular states via their electromagnetic properties. The angular amplitude analyses of the final-state hadrons may provide crucial information to disentangle different spin-parity quantum numbers. We hope further experiments can bring us more surprises.

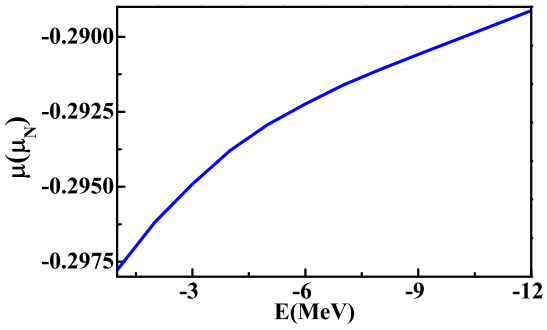

FIG. 5. The transition magnetic moment of the $\Xi_c'\bar{D}^*|3/2^-\rangle \to \Xi_c'\bar{D}^*|1/2^-\rangle\gamma$ process dependent on the binding energies of the isoscalar $\Xi_c'\bar{D}^*$ molecular states with $J^P = (1/2^-, 3/2^-)$ after considering the S-D wave mixing effect.

IV. SUMMARY

In the past few years, the community has made big progress on exploring the hidden-charm molecular pentaquarks [2,6–12]. Especially, the observaton of three P_ψ^N states in 2019 [13] provides a strong evidence of the existence of the hidden-charm molecular pentaquark states in the hadron spectroscopy [14–20]. Recently, the reported evidence of the $P_{\psi s}^\Lambda(4459)$ [21] and the observation of the $P_{\psi s}^\Lambda(4338)$ [49] may provide us a good opportunity to identify the hidden-charm molecular pentaquarks with strangeness. In Refs. [51,52], the characteristic mass spectrum of S-wave $\Xi_c^{(\prime)}\bar{D}^{(*)}$-type hidden-charm molecular pentaquarks with strangeness was proposed, which is stimulated by the $P_{\psi s}^\Lambda(4459)$ [21] and $P_{\psi s}^\Lambda(4338)$ [49]. However, other properties of the S-wave isoscalar $\Xi_c^{(\prime)}\bar{D}^{(*)}$ molecular states are still waiting to be further discussed, which can provide further information to reflect the inner structures of these discussed S-wave isoscalar $\Xi_c^{(\prime)}\bar{D}^{(*)}$ molecular pentaquarks.

In this work, we study the electromagnetic properties of the S-wave isoscalar $\Xi_c^{(\prime)}\bar{D}^{(*)}$ molecular states through the constituent quark model. In the concrete calculation, we first focus on the magnetic moments of the S-wave isoscalar $\Xi_c^{(\prime)}\bar{D}^{(*)}$ molecular states. Our numerical results show that the magnetic moment of the S-wave isoscalar $\Xi_c^{(\prime)}\bar{D}^*$ molecule with $J^P = 1/2^-$ is obviously different from that of the S-wave isoscalar $\Xi_c^{(\prime)}\bar{D}^*$ molecule with $J^P = 3/2^-$. Thus, measuring the magnetic moments of them is an effective approach to reflect their underlying structures. After that, we extend our theoretical framework to study the transition magnetic moments between the S-wave isoscalar $\Xi_c^{(\prime)}\bar{D}^{(*)}$ molecular states. And then, we find several relations of the transition magnetic moments. Especially, the transition magnetic moments of the S-wave isoscalar $\Xi_c^{(\prime)}\bar{D}^*$ molecules with $J^P = 1/2^-$ and $J^P = 3/2^-$ are different. After obtaining the transition magnetic moments between the S-wave isoscalar $\Xi_c^{(\prime)}\bar{D}^{(*)}$ molecular states, we also discuss the radiative decay behaviors between the S-wave isoscalar $\Xi_c^{(\prime)}\bar{D}^{(*)}$ molecular states, where most of the radiative decay widths between the S-wave isoscalar $\Xi_c^{(\prime)}\bar{D}^{(*)}$ molecules are around 5.0 keV. Finally, we discuss the electromagnetic properties of the isoscalar $\Xi_c^{(\prime)}\bar{D}^{(*)}$ molecular states by considering the S-D wave mixing effect [52]. When making comparison of the numerical results with and without the S-D wave mixing effect, we find that the S-D wave mixing effect plays a rather minor role for the magnetic moments of the isoscalar $\Xi_c'\bar{D}^*$ molecular states with $J^P = 1/2^-$ and $J^P = 3/2^-$ and the transition magnetic moment of the $\Xi_c'\bar{D}^*|3/2^-\rangle \to \Xi_c'\bar{D}^*|1/2^-\rangle\gamma$ process, since the components of the D-wave channels are not dominant for these states [52].

In summary, although the hadronic molecular states have attracted much attention on both the theoretical and experimental sides [2–12], investigation of the electromagnetic properties of the hadronic molecules has not received plenty of attention. In this work, we are dedicated to this issue. We hope that the present work can stimulate further experimental and theoretical exploration of the electromagnetic properties of the hadronic molecular states.

ACKNOWLEDGMENTS

This work is supported by the China National Funds for Distinguished Young Scientists under Grant No. 11825503, National Key Research and Development Program of China under Contract No. 2020YFA0406400, the 111 Project under Grant No. B20063, and the National Natural Science Foundation of China under Grant Nos. 12175091, 11965016, and 12047501.

[1] S. K. Choi *et al.* (Belle Collaboration), Observation of a Narrow Charmonium-like State in Exclusive $B^{\pm} \to K^{\pm}\pi^{+}\pi^{-}J/\psi$ Decays, Phys. Rev. Lett. **91**, 262001 (2003).
[2] N. Brambilla, S. Eidelman, C. Hanhart, A. Nefediev, C. P. Shen, C. E. Thomas, A. Vairo, and C. Z. Yuan, The XYZ states: Experimental and theoretical status and perspectives, Phys. Rep. **873**, 1 (2020).
[3] X. Liu, An overview of XYZ new particles, Chin. Sci. Bull. **59**, 3815 (2014).
[4] A. Hosaka, T. Iijima, K. Miyabayashi, Y. Sakai, and S. Yasui, Exotic hadrons with heavy flavors: X, Y, Z, and related states, Prog. Theor. Exp. Phys. **2016**, 062C01 (2016).
[5] H. X. Chen, W. Chen, X. Liu, and S. L. Zhu, The hidden-charm pentaquark and tetraquark states, Phys. Rep. **639**, 1 (2016).
[6] J. M. Richard, Exotic hadrons: Review and perspectives, Few Body Syst. **57**, 1185 (2016).
[7] R. F. Lebed, R. E. Mitchell, and E. S. Swanson, Heavy-quark QCD exotica, Prog. Part. Nucl. Phys. **93** (2017), 143–194.
[8] S. L. Olsen, T. Skwarnicki, and D. Zieminska, Nonstandard heavy mesons and baryons: Experimental evidence, Rev. Mod. Phys. **90**, 015003 (2018).
[9] F. K. Guo, C. Hanhart, U. G. Meißner, Q. Wang, Q. Zhao, and B. S. Zou, Hadronic molecules, Rev. Mod. Phys. **90**, 015004 (2018).
[10] Y. R. Liu, H. X. Chen, W. Chen, X. Liu, and S. L. Zhu, Pentaquark and tetraquark states, Prog. Part. Nucl. Phys. **107**, 237 (2019).
[11] L. Meng, B. Wang, G. J. Wang, and S. L. Zhu, Chiral perturbation theory for heavy hadrons and chiral effective field theory for heavy hadronic molecules, arXiv: 2204.08716.
[12] H. X. Chen, W. Chen, X. Liu, Y. R. Liu, and S. L. Zhu, An updated review of the new hadron states, arXiv:2204.02649.
[13] R. Aaij *et al.* (LHCb Collaboration), Observation of a Narrow Pentaquark State, $P_c(4312)^+$, and of Two-Peak Structure of the $P_c(4450)^+$, Phys. Rev. Lett. **122**, 222001 (2019).
[14] J. J. Wu, R. Molina, E. Oset, and B. S. Zou, Prediction of Narrow N^* and Λ^* Resonances with Hidden Charm Above 4 GeV, Phys. Rev. Lett. **105**, 232001 (2010).
[15] W. L. Wang, F. Huang, Z. Y. Zhang, and B. S. Zou, $\Sigma_c\bar{D}$ and $\Lambda_c\bar{D}$ states in a chiral quark model, Phys. Rev. C **84**, 015203 (2011).
[16] Z. C. Yang, Z. F. Sun, J. He, X. Liu, and S. L. Zhu, The possible hidden-charm molecular baryons composed of anti-charmed meson and charmed baryon, Chin. Phys. C **36**, 6 (2012).
[17] J. J. Wu, T.-S. H. Lee, and B. S. Zou, Nucleon resonances with hidden charm in coupled-channel models, Phys. Rev. C **85**, 044002 (2012).
[18] X. Q. Li and X. Liu, A possible global group structure for exotic states, Eur. Phys. J. C **74**, 3198 (2014).
[19] R. Chen, X. Liu, X. Q. Li, and S. L. Zhu, Identifying Exotic Hidden-Charm Pentaquarks, Phys. Rev. Lett. **115**, 132002 (2015).
[20] M. Karliner and J. L. Rosner, New Exotic Meson and Baryon Resonances from Doubly-Heavy Hadronic Molecules, Phys. Rev. Lett. **115**, 122001 (2015).
[21] R. Aaij *et al.* (LHCb Collaboration), Evidence of a $J/\psi\Lambda$ structure and observation of excited Ξ^- states in the $\Xi_b^- \to J/\psi\Lambda K^-$ decay, Sci. Bull. **66**, 1278 (2021).
[22] J. Hofmann and M. F. M. Lutz, Coupled-channel study of crypto-exotic baryons with charm, Nucl. Phys. **A763**, 90 (2005).
[23] J. J. Wu, R. Molina, E. Oset, and B. S. Zou, Dynamically generated N^* and Λ^* resonances in the hidden charm sector around 4.3 GeV, Phys. Rev. C **84**, 015202 (2011).
[24] V. V. Anisovich, M. A. Matveev, J. Nyiri, A. V. Sarantsev, and A. N. Semenova, Nonstrange and strange pentaquarks with hidden charm, Int. J. Mod. Phys. A **30**, 1550190 (2015).
[25] Z. G. Wang, Analysis of the $\frac{1}{2}^{\pm}$ pentaquark states in the diquark-diquark-antiquark model with QCD sum rules, Eur. Phys. J. C **76**, 142 (2016).
[26] A. Feijoo, V. K. Magas, A. Ramos, and E. Oset, A hidden-charm $S = -1$ pentaquark from the decay of Λ_b into $J/\psi\eta\Lambda$ states, Eur. Phys. J. C **76**, 446 (2016).
[27] J. X. Lu, E. Wang, J. J. Xie, L. S. Geng, and E. Oset, The $\Lambda_b \to J/\psi K^0\Lambda$ reaction and a hidden-charm pentaquark state with strangeness, Phys. Rev. D **93**, 094009 (2016).
[28] H. X. Chen, L. S. Geng, W. H. Liang, E. Oset, E. Wang, and J. J. Xie, Looking for a hidden-charm pentaquark state with strangeness $S = -1$ from Ξ_b^- decay into $J/\psi K^-\Lambda$, Phys. Rev. C **93**, 065203 (2016).

[29] R. Chen, J. He, and X. Liu, Possible strange hidden-charm pentaquarks from $\Sigma_c^{(*)}\bar{D}_s^*$ and $\Xi_c^{(\prime,*)}\bar{D}^*$ interactions, Chin. Phys. C **41**, 103105 (2017).

[30] X. Z. Weng, X. L. Chen, W. Z. Deng, and S. L. Zhu, Hidden-charm pentaquarks and P_c states, Phys. Rev. D **100**, 016014 (2019).

[31] C. W. Xiao, J. Nieves, and E. Oset, Prediction of hidden charm strange molecular baryon states with heavy quark spin symmetry, Phys. Lett. B **799**, 135051 (2019).

[32] C. W. Shen, H. J. Jing, F. K. Guo, and J. J. Wu, Exploring possible triangle singularities in the $\Xi_b^- \to K^- J/\psi\Lambda$ decay, Symmetry **12**, 1611 (2020).

[33] B. Wang, L. Meng, and S. L. Zhu, Spectrum of the strange hidden charm molecular pentaquarks in chiral effective field theory, Phys. Rev. D **101**, 034018 (2020).

[34] Q. Zhang, B. R. He, and J. L. Ping, Pentaquarks with the $qqs\bar{Q}Q$ configuration in the chiral quark model, arXiv:2006.01042.

[35] H. X. Chen, W. Chen, X. Liu, and X. H. Liu, Establishing the first hidden-charm pentaquark with strangeness, Eur. Phys. J. C **81**, 409 (2021).

[36] F. Z. Peng, M. J. Yan, M. Sánchez Sánchez, and M. P. Valderrama, The $P_{cs}(4459)$ pentaquark from a combined effective field theory and phenomenological perspectives, Eur. Phys. J. C **81**, 666 (2021).

[37] R. Chen, Can the newly reported $P_{cs}(4459)$ be a strange hidden-charm $\Xi_c\bar{D}^*$ molecular pentaquark?, Phys. Rev. D **103**, 054007 (2021).

[38] H. X. Chen, Hidden-charm pentaquark states through the current algebra: From their productions to decays, Chin. Phys. C **46**, 093105 (2022).

[39] M. Z. Liu, Y. W. Pan, and L. S. Geng, Can discovery of hidden charm strange pentaquark states help determine the spins of $P_c(4440)$ and $P_c(4457)$?, Phys. Rev. D **103**, 034003 (2021).

[40] C. W. Xiao, J. J. Wu, and B. S. Zou, Molecular nature of $P_{cs}(4459)$ and its heavy quark spin partners, Phys. Rev. D **103**, 054016 (2021).

[41] M. L. Du, Z. H. Guo, and J. A. Oller, Insights into the nature of the $P_{cs}(4459)$, Phys. Rev. D **104**, 114034 (2021).

[42] J. T. Zhu, L. Q. Song, and J. He, $P_{cs}(4459)$ and other possible molecular states from $\Xi_c^{(*)}\bar{D}^{(*)}$ and $\Xi_c'\bar{D}^{(*)}$ interactions, Phys. Rev. D **103**, 074007 (2021).

[43] X. K. Dong, F. K. Guo, and B. S. Zou, A survey of heavy-antiheavy hadronic molecules, Progr. Phys. **41**, 65 (2021).

[44] K. Chen, R. Chen, L. Meng, B. Wang, and S. L. Zhu, Systematics of the heavy flavor hadronic molecules, Eur. Phys. J. C **82**, 581 (2022).

[45] R. Chen and X. Liu, Mass behavior of hidden-charm open-strange pentaquarks inspired by the established P_c molecular states, Phys. Rev. D **105**, 014029 (2022).

[46] K. Chen, B. Wang, and S. L. Zhu, Heavy flavor molecular states with strangeness, Phys. Rev. D **105**, 096004 (2022).

[47] X. Hu and J. Ping, Investigation of hidden-charm pentaquarks with strangeness $S = -1$, Eur. Phys. J. C **82**, 118 (2022).

[48] R. Aaij *et al.* (LHCb Collaboration), Observation of J/ψ Resonances Consistent with Pentaquark States in $\Lambda_b^0 \to J/\psi K^- p$ Decays, Phys. Rev. Lett. **115**, 072001 (2015).

[49] Chen Chen and Elisabetta Spadaro on behalf of the LHCb Collaboration, Particle Zoo 2.0: New tetra- and pentaquarks at LHCb, LHC Seminar, https://indico.cern.ch/event/1176505/.

[50] X. W. Wang and Z. G. Wang, Analysis of the $P_{cs}(4338)$ and related pentaquark molecular states via the QCD sum rules, arXiv:2207.06060.

[51] M. Karliner and J. R. Rosner, strange pentaquarks, Phys. Rev. D **106**, 036024 (2022).

[52] F. L. Wang and X. Liu, Emergence of molecular-type characteristic spectrum of hidden-charm pentaquark with strangeness embodied in the $P_{\psi s}^{\Lambda}(4338)$ and $P_{cs}(4459)$, arXiv:2207.10493.

[53] M. J. Yan, F. Z. Peng, M. S. Sánchez, and M. Pavon Valderrama, The $P_{\psi s}^{\Lambda}(4338)$ pentaquark and its partners in the molecular picture, arXiv:2207.11144.

[54] L. Meng, B. Wang, and S. L. Zhu, The double thresholds distort the lineshapes of the $P_{\psi s}^{\Lambda}(4338)^0$ resonance, arXiv:2208.03883.

[55] G. J. Wang, R. Chen, L. Ma, X. Liu, and S. L. Zhu, Magnetic moments of the hidden-charm pentaquark states, Phys. Rev. D **94**, 094018 (2016).

[56] M. W. Li, Z. W. Liu, Z. F. Sun, and R. Chen, Magnetic moments and transition magnetic moments of P_c and P_{cs} states, Phys. Rev. D **104**, 054016 (2021).

[57] F. Schlumpf, Magnetic moments of the baryon decuplet in a relativistic quark model, Phys. Rev. D **48**, 4478 (1993).

[58] G. Ramalho, K. Tsushima, and F. Gross, A relativistic quark model for the Omega-electromagnetic form factors, Phys. Rev. D **80**, 033004 (2009).

[59] Y. R. Liu, P. Z. Huang, W. Z. Deng, X. L. Chen, and S. L. Zhu, Pentaquark magnetic moments in different models, Phys. Rev. C **69**, 035205 (2004).

[60] C. Deng and S. L. Zhu, T_{cc}^+ and its partners, Phys. Rev. D **105**, 054015 (2022).

[61] F. Gao and H. S. Li, Magnetic moments of the hidden-charm strange pentaquark states, arXiv:2112.01823.

[62] H. Y. Zhou, F. L. Wang, Z. W. Liu, and X. Liu, Probing the electromagnetic properties of the $\Sigma_c^{(*)}D^{(*)}$-type doubly charmed molecular pentaquarks, Phys. Rev. D **106**, 034034 (2022).

[63] U. Ozdem, Investigation of magnetic moment of $P_{cs}(4338)$ and $P_{cs}(4459)$ molecular pentaquarks, arXiv:2208.07684.

[64] P. Z. Huang, Y. R. Liu, W. Z. Deng, X. L. Chen, and S. L. Zhu, Heavy pentaquarks, Phys. Rev. D **70**, 034003 (2004).

[65] V. Šimonis, Magnetic properties of ground-state mesons, Eur. Phys. J. A **52**, 90 (2016).

[66] R. L. Workman *et al.* (Particle Data Group), Review of Particle Physics, Prog. Theor. Exp. Phys. **2022**, 083C01 (2022).

[67] S. Kumar, R. Dhir, and R. C. Verma, Magnetic moments of charm baryons using effective mass and screened charge of quarks, J. Phys. G **31**, 141 (2005).

[68] A. Faessler, T. Gutsche, M. A. Ivanov, J. G. Korner, V. E. Lyubovitskij, D. Nicmorus, and K. Pumsa-ard, Magnetic moments of heavy baryons in the relativistic three-quark model, Phys. Rev. D **73**, 094013 (2006).

[69] L. Y. Glozman and D. O. Riska, The Charm and bottom hyperons and chiral dynamics, Nucl. Phys. **A603**, 326 (1996); **A620**, 510 (1997).

[70] V. Simonis, Improved predictions for magnetic moments and M1 decay widths of heavy hadrons, arXiv:1803.01809.
[71] T. M. Aliev, K. Azizi, and A. Ozpineci, Magnetic moments of heavy Ξ_Q baryons in light cone QCD sum rules, Phys. Rev. D **77**, 114006 (2008).
[72] T. M. Aliev, T. Barakat, and M. Savci, Magnetic moments of heavy $J^P = \frac{1}{2}^+$ baryons in light cone QCD sum rules, Phys. Rev. D **91**, 116008 (2015).
[73] B. Wang, B. Yang, L. Meng, and S. L. Zhu, Radiative transitions and magnetic moments of the charmed and bottom vector mesons in chiral perturbation theory, Phys. Rev. D **100**, 016019 (2019).
[74] S. K. Bose and L. P. Singh, Magnetic moments of charmed and B flavored hadrons in MIT bag Model, Phys. Rev. D **22**, 773 (1980).
[75] A. Hazra, S. Rakshit, and R. Dhir, Radiative M1 transitions of heavy baryons: Effective quark mass scheme, Phys. Rev. D **104**, 053002 (2021).
[76] A. Girdhar, H. Dahiya, and M. Randhawa, Magnetic moments of $J^P = \frac{3}{2}^+$ decuplet baryons using effective quark masses in chiral constituent quark model, Phys. Rev. D **92**, 033012 (2015).
[77] J. Franklin, D. B. Lichtenberg, W. Namgung, and D. Carydas, Wave function mixing of flavor degenerate baryons, Phys. Rev. D **24**, 2910 (1981).
[78] J. Dey, V. Shevchenko, P. Volkovitsky, and M. Dey, Radiative decays of S-wave charmed baryons, Phys. Lett. B **337**, 185 (1994).
[79] T. Barnes, S. Godfrey, and E. S. Swanson, Higher charmonia, Phys. Rev. D **72**, 054026 (2005).